



Towards finding structure in a chaotic sea of light

THESIS

submitted in partial fulfillment of the
requirements for the degree of

BACHELOR OF SCIENCE

in

PHYSICS AND ASTRONOMY

Author :	Jonathan Pilgram
Student ID :	s1855670
Supervisor :	Dr. Wolfgang Löffler
2 nd corrector :	Dr. in. Frans Snik

Leiden, The Netherlands, April 14, 2020

Towards finding structure in a chaotic sea of light

Jonathan Pilgram (s1855670)
First supervisor: Dr. Wolfgang Löffler
Second supervisor: Dr. in. Frans Snik
Leiden University

April 14, 2020

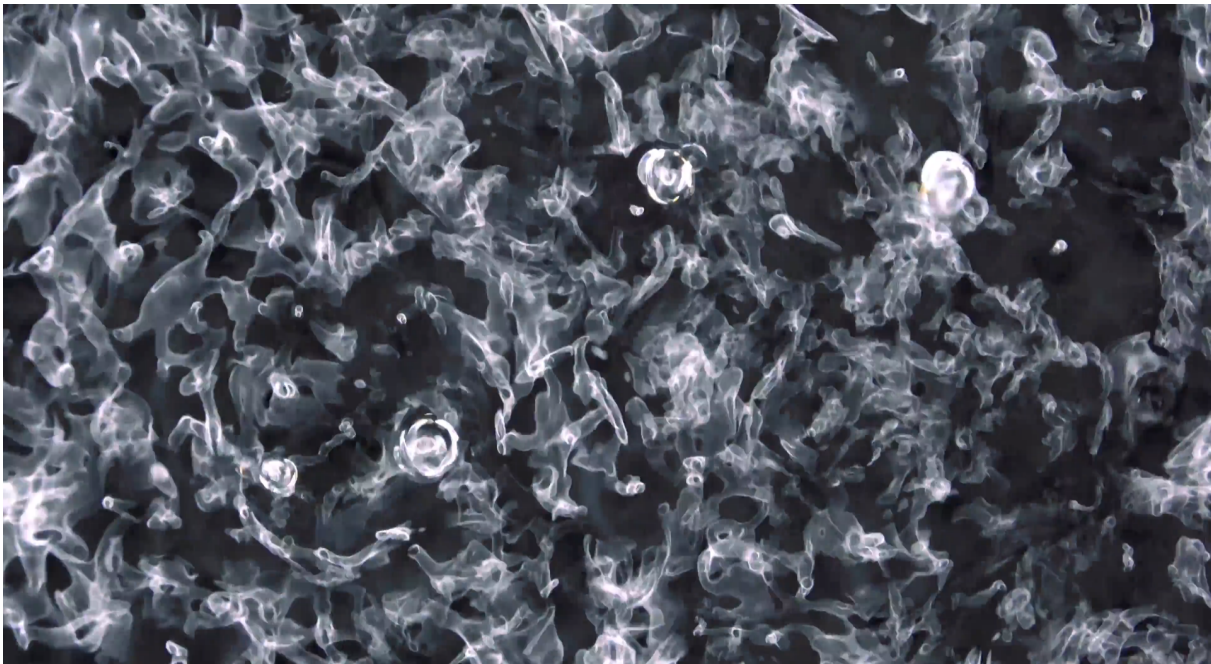


Figure 1: Still from Decoherence, an audiovisual composition from Paloma Kop, 2019. <https://palomakop.tv/Decoherence>

Abstract

Can fluctuations be found in visible thermal light? To answer this three sections of literature research are included in which the following subjects will be explored: Spatial/temporal modes/coherence, stellar interferometry and the second order correlation function ($g^{(2)}$) for thermal light. The insights gained in these sections will be used for two experiments. The first experiment is designed to detect spatial fluctuations, which was achieved by a simple setup involving a double slit and two pinholes. The second experiment, designed to detect temporal fluctuations using the $g^{(2)}$ of a quasi-thermal light source, did not find significant results, which contradicts the results of a simulation of $g^{(2)}$ for thermal light.

Acknowledgments

First of all I would like to acknowledge and thank my first supervisor, Wolfgang Löffler, for the time he has put into the project and me. He gave me the supervision that is normally expected for a PhD student. At times this seemed a double edged sword as he also expected me to be on the level of a PhD student, but I could not have wished for a more committed supervisor.

I would like to thank Lotte-Sophie Groenendijk not only for proofreading of this thesis, but also for all the moral support and patience during my research project.

I would like to thank Tomas Ostenholt for rehearsing the presentation of this thesis and for the interesting conversations.

I would like to thank Benjamin van Ommen, Ivar and Mio Poortvliet for proofreading of the thesis.

And at last, I would like to thank all the people from the quantum optics group for the interesting talks at lunch, the help they provided with the research and the fun we had at the group events.

Contents

Acknowledgments	2
Introduction	4
Spatial versus temporal modes	4
Coherence and incoherence	6
Stellar interferometry	9
Van Cittert-Zernike theorem	10
Photons per mode of a thermal light source	11
Experiment: Spatial fluctuations	12
Prediction	13
Results	14
Discussion	14
Second order correlation function	16
Correlation of thermal light	16
Fabry-Pérot filter	17
Experiment: Temporal fluctuations	19
Numeric simulation	21
Experimental results	25
Discussion	28
Conclusion	30
References	31
Appendix A: List of experimental equipment	32
Appendix B: Second order correlation function simulation code	33

Introduction

Towards finding structure in a chaotic sea of light is the title of this bachelor research. Structure in light will mean that the light waves are predictable and fluctuations caused by the phase of the light will be visible. Chaotic light waves on the other hand are impossible to perfectly predict and all fluctuations will average away. Structure and chaos in the context of light will be the main focus of this research.

The title can be rephrased in a more scientific manner: Can fluctuations be found in visible thermal light? As we will soon learn there are mainly two kinds of fluctuations in light, being spatial and temporal fluctuations. As of such the question above requires an answer in twofold. It first will be answered for spatial fluctuations, followed by temporal fluctuations.

Because of the nonstandard twofold answer, the research has also been structured in a nonstandard way. The introduction will continue with an introduction to modal theory of light. In which spatial/temporal modes/coherence will be explained. Then theory and experiments will be alternated. A theory chapter about stellar interferometry (a way to use spatial fluctuations to find the size of distant objects) will be presented, directly followed by an experiment designed to find spatial fluctuations. Then, the second order correlation function (for thermal light) will be presented. This is then followed by an experiment designed to find temporal fluctuations. Finally, a conclusion will be given on the question: Can fluctuations be found in visible thermal light?

Spatial versus temporal modes

Underlying the whole thesis is the concept of (optical) modes. Any homogeneously polarized two-dimensional light field that is observed can be decomposed into a set of infinite independent spatial modes. An example of two orthogonal bases for spatial modes of light are the Laguerre-Gauss and Hermite-Gauss bases.

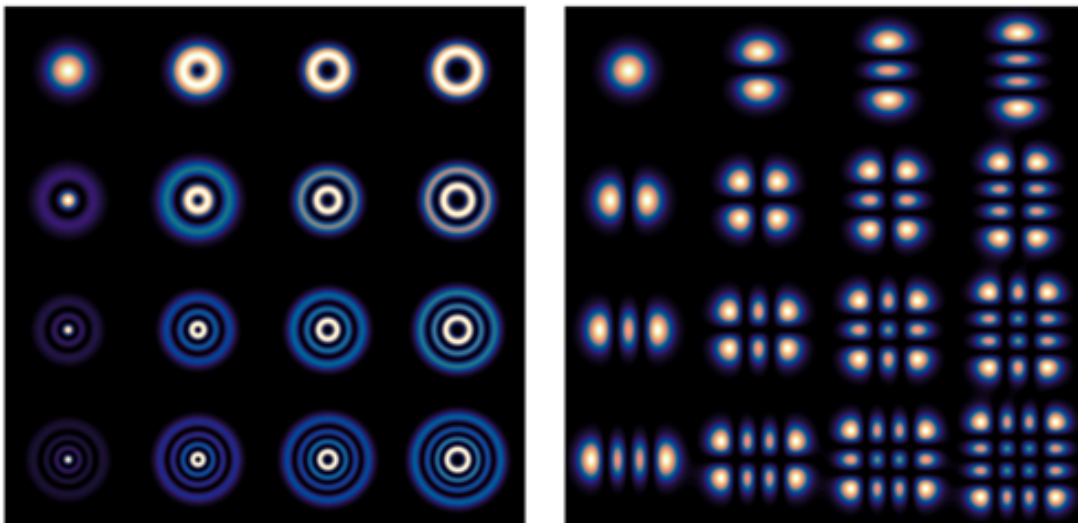


Figure 2: Left: Laguerre-Gauss modes. Right: Hermite-Gauss modes. Both are a complete, but different, orthogonal spatial basis for light. In the upper-left corner is the $|00\rangle$ mode for both figures (Gaussian beam). From left to right shown are the $|00\rangle, |01\rangle, |02\rangle, \dots$ modes. From top to bottom the $|00\rangle, |10\rangle, |20\rangle, \dots$ modes.¹

Important to note is that in these bases the modes are independent, meaning that a superposition of two modes can exist ($\frac{1}{2} |00\rangle + \frac{1}{2} |01\rangle$). The modes can be converted from one basis to another. Example: Light can be converted from a Hermite-Gauss to Laguerre-Gauss basis. However *the amount of photons in a mode cannot increase* without the use of active optical elements. Maybe more important to note is that Hermite-Gauss and Laguerre-Gauss are only representations of spatial modes. There exists a totally different kind of modes, named temporal modes. We will now go over the differences and similarities between spatial and temporal modes:

	Spatial modes	Temporal modes
Smallest measurable unit	Coherence area (Diffraction limit)	Photon bandwidth (Wiener-Khinchin theorem)
Invariant product	Source area · solid angle (Etendue)	Spectral width · temporal width (Time-bandwidth product)
Defined by	Spatial coherence	Temporal coherence
Filtering	Spatial apertures (Van Cittert-Zernike)	Spectral filter (colored glass, optical cavity etc.)
Single mode filter	Optical fiber	Lifetime-limited atomic transition

Table 1: Summary of differences and similarities of spatial and temporal modes.

Let us go over the differences stated in the table. First spatial modes will be defined, after which temporal modes will be explained. At the end the differences and similarities become clear. A spatial mode is the smallest difference in the direction of a wave vector that can be observed by a certain experimental setup. This smallest observable difference is defined by the diffraction limit:

$$\theta = 1.22 \frac{\lambda}{D} \quad (1)$$

In which θ is the angular resolution of the setup or the smallest difference of a wave vector that can be observed by the setup. λ is the wavelength of the light. D is the diameter of the opening of the setup. The factor 1.22 can change a bit depending on the shape of the opening, however it will always be of the same order. From this can be inferred that the product of the source size (in units wavelength) and the solid angle will remain constant for a single spatial mode. (And is equal to 1.22 for a circular source.) This is closely related to étendue, which is size of a beam given in steradians. (Grynberg, Aspect, & Alain, 2010) The étendue can only stay the same or increase, which can be inverted to make the earlier statement: The amount of photons per mode can only stay the same or decrease. All of this is closely related to spatial coherence, which we will cover in depth in the next section.

The relation between spectral bandwidth and temporal length of the wave packet is given by the Wiener-Khinchin theorem (Daendliker, 2000):

$$\Gamma(\tau) = \int_{-\infty}^{\infty} S(\nu) e^{2i\pi\nu\tau} d\nu \quad (2)$$

This relates the temporal correlation function $\Gamma(\tau)$ to the power-spectral density $S(\nu)$ via a Fourier transform. ν is the frequency and τ is the time delay. The smallest difference that can be measured is defined by the spacing between the zeros of the correlation function. From this is found that for one temporal mode the product of the spectral width and temporal width must remain constant (and is equal to 0.44 for a Gaussian shaped spectrum). This product is also called the

¹Figure provided by Guido Stam, Universiteit Leiden, 27 November 2019

time-bandwidth product. Temporal modes are closely related to temporal coherence, which will be covered in the next section.

To filter the amount of spatial modes observed a simple pinhole can be used. A pinhole effectively decreases the size of the source, which in turn must increase the solid angle of the individual spatial modes. The amount of modes observed also decreases if the distance to the source is increased. This is best described by the van Cittert-Zernike theorem. (See: Van Cittert-Zernike theorem) Filtering of temporal modes can be achieved by decreasing the frequency/wavelength range observed. A simple spectral filter can be used, such as colored piece of glass. However to really narrow the spectrum down to a level at which only a few temporal modes are observed, a Fabry-Pérot cavity must be used. (See: Fabry-Pérot filter)

Obtaining a single spatial mode is trivial nowadays. Light can simply be coupled into a single mode fiber. At the other end of the fiber exactly one spatial mode will be observed. However measuring a single temporal mode for visible light is far from trivial as the frequency of visible light is in the order of 10^{15} Hz. So, as will be explained more in depth during the next section, to easily measure a single temporal mode a camera of comparable frequency is required. Such a camera of course does not exist (normal high-speed cameras go up to about one MHz), so filtering is required in order to measure a single temporal mode.

Spatial and temporal modes are similar in the properties that they both form a discrete orthogonal basis for describing light. Most properties of spatial modes have similar counterpart for temporal modes, however the two kinds of modes are very different. Spatial modes will always in some way depend on the spatial dimensions of the setup and source, while temporal modes will depend on the time window of the measurement and the spectrum. The key difference will now be further explored for two closely related concepts, namely spatial and temporal coherence.

Coherence and incoherence

In this section the following definition of a wavetrain will be used: The electric field is described by the analytic signal $U(r, t)$ (which is assumed to be a superposition of different frequencies). $U(r, t)$ is defined as the amplitude of the wave at location r and time t . Now a wavetrain is defined as the whole wave $U(r)$ passing through a fixed r as a function of t . (Brooker, 2003, p. 194-195)

Coherence of light is the predictability of these wavetrain(s) for observed light. If a perfectly coherent wavetrain is observed, then it is possible to predict the amplitude of the magnetic and electric field everywhere. However more incoherent wavetrains are more randomized. The result of an incoherent wavetrain is a scrambled signal of which it is impossible to predict the amplitude of the fields correctly after a certain coherence time or distance. There are two kinds of coherence, which are independent of each other. The first being spatial coherence and the second being temporal coherence. They both will now be introduced.

Spatial coherence is defined as the correlation between the complex electromagnetic wavetrains measured at two points. This can be formalized by the spatial coherence/correlation function:

$$\Gamma(\mathbf{r}_1, \mathbf{r}_2, t) = \overline{U^*(\mathbf{r}_1, t)U(\mathbf{r}_2, t)} \quad (3)$$

Where $U^*(\mathbf{r}_1, t)$ is the conjugate of the complex amplitude measured at \mathbf{r}_1 at time t and $U(\mathbf{r}_2, t)$ is the complex amplitude measured at \mathbf{r}_2 at the same time t . The bar denotes time averaging. If the function is normalized correctly, then the value will range between 0 (perfect incoherence) and 1 (perfect coherence). Coherence distance can now be defined. This is the distance for which the spatial coherence decreases by a factor of $\frac{1}{e}$ and is given by:

$$d_c = \frac{\lambda}{\theta} \quad (4)$$

In which λ is the wavelength and θ is the angular size of the source. Spatial coherence can be measured by looking the interference pattern created by Young's slit experiment.

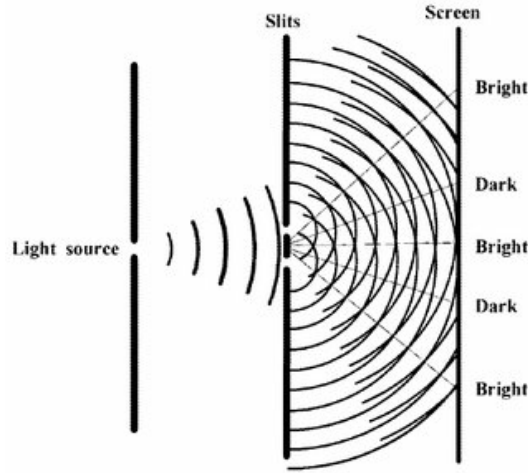


Figure 3: Basic schematic of a Young's double slit experiment. Light is send through two slits, which creates an interference pattern on the screen.²

The visibility of the resulting interference pattern is dependent on the normalized spatial coherence function of the incoming light in the following way:

$$|\Gamma(\mathbf{r}_1, \mathbf{r}_2, t)| = \frac{I_{max} - I_{min}}{I_{max} + I_{min}} \quad (5)$$

I_{max} is the maximum of intensity measured in the interference pattern and I_{min} is the minimum intensity found. This result can be explained by the following reasoning: If there is almost perfect spatial coherence, than the phase of the wavetrain is well defined at every point in space and so is the interference pattern. However if there is almost no spatial coherence, then the phase will be almost random at every point in space. This results in adding waves with a random phase differences, which results in an average constant intensity. (Brooker, 2003)

Temporal coherence is on the other hand is the correlation of a wavetrain measured at two different moments in time. This is given by the autocorrelation/temporal coherence function:

$$\Gamma(\mathbf{r}, t, \tau) = \overline{U^*(\mathbf{r}, t)U(\mathbf{r}, t + \tau)} \quad (6)$$

Which is dependent on the complex amplitude $U(\mathbf{r}, t)$ measured at the place \mathbf{r} and time t and is correlated with the complex amplitude of $t + \tau$. A coherence time can now be defined, which is the times it takes before the temporal coherence function drops by a factor of $\frac{1}{e}$:

$$\tau_c = \frac{1}{\Delta\nu} \quad (7)$$

$\Delta\nu$ is the spectral bandwidth of the light field. This can be multiplied by the speed of light c to define the coherence length:

$$l_c = c\tau_c \quad (8)$$

²Source figure: Who invented Young's Modulus? - Scientific Figure on ResearchGate. Available from: https://www.researchgate.net/figure/interference-Youngs-double-slit-method-His-interest-in-wave-behaviour-led-him-also-to_fig2_26504488 [accessed 26 Feb, 2020]

Temporal coherence is also known as the longitudinal coherence. (Mandel & Wolf, 1995) Spatial and temporal coherence are independent, which is best exemplified by a interference pattern created with sunlight (broad spectrum). In the figure below it is visible that after letting sunlight pass through a double slit, a clearly visible interference pattern is created. This is because the spatial coherence of the light at the two slits is high. The spectrum is broad, so the temporal coherence on the other hand must be very low. From this experiment can be concluded that spatial coherence is independent of temporal coherence.

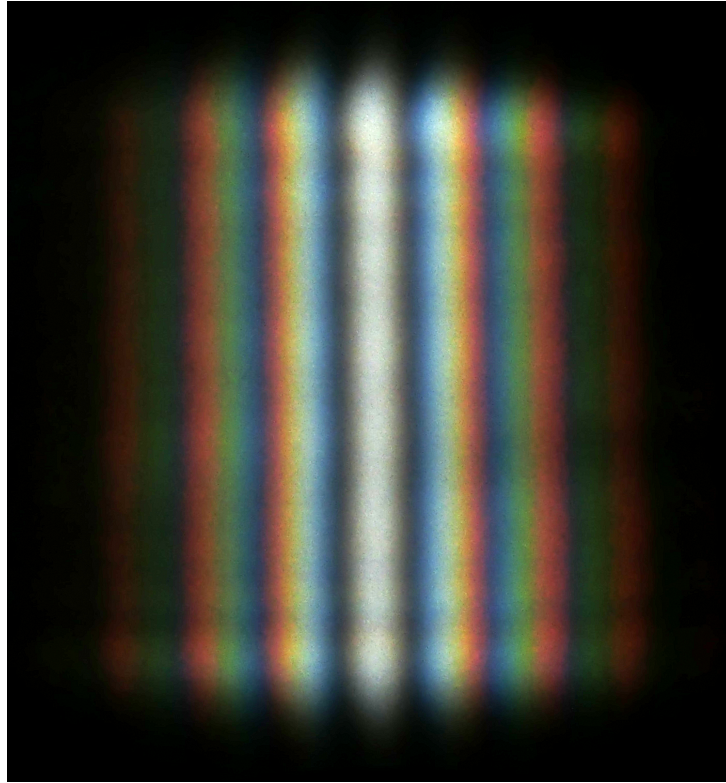


Figure 4: Interference pattern of sunlight. Created by using a double slit. Visible is the high contrast of the pattern, but also the broad spectrum of light. This indicates a high spatial coherence, but a low temporal coherence.³

Just like there are two kinds of optical modes (spatial and temporal), there are also two kinds of coherence. Spatial coherence which can be described with a correlation function. Temporal coherence is described by an autocorrelation function. The coherence length gives a definition for spatial modes. Coherence time, on the other hand, gives a definition for temporal modes. Using this we find that the visibility of interference fringes can be described by the amount of modes observed.

*For the beginners in the field of optical coherence the following book is advised, as it very clearly explains the basis of coherence:
Modern Classical Optics - Geoffrey Brooker - 2003*

³By Aleksandr Berdnikov - Own work, CC BY-SA 4.0, <https://commons.wikimedia.org/w/index.php?curid=53009002>

Stellar interferometry

In 1921 was, for the first time in human history, the size of an extrasolar star determined. This was done by Michelson using a stellar interferometer. The size of the star Betelgeuze was determined, which is at a distance of $6 \cdot 10^{18}$ m and has a diameter of $1.2 \cdot 10^{11}$ m. (Michelson & Pease, 1921) This section will explain how Michelson used the properties of spatial coherence and spatial modes to determine the size of Betelgeuze.

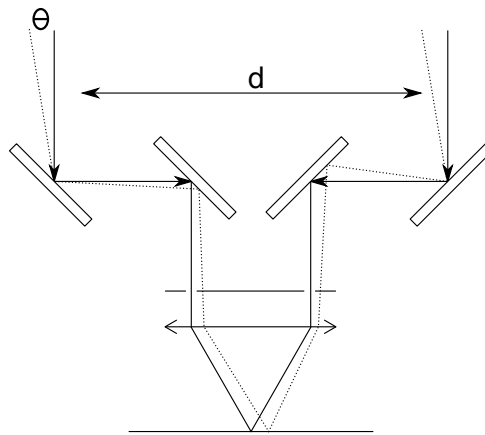


Figure 5: Schematic of a Michelson stellar interferometer. Two incident light fields from an acceptance angle θ are collected by mirrors spaced a distance d from each other. These light beams are then interfered in order to observe an interference pattern. This setup was used in 1921 to determine the size of Betelgeuze.

Above is a schematic drawing of the setup Michelson used. This is basically a double slit experiment, so an interference pattern can be observed. By using the two different light paths for the slits, he could effectively choose the distance between the slits. If the mirrors are very close together (much closer than the coherence length of the light of the observed object), a very high visibility for the interference pattern is to be expected. However if the distance becomes larger than the coherence length, then the visibility will be reduced. This is shown in the figure below.

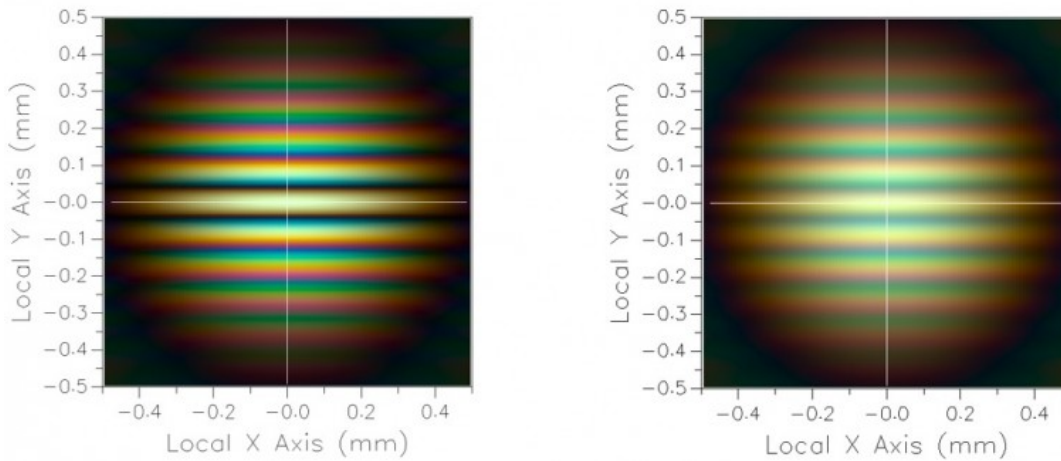


Figure 6: Resulting interference patterns of a Michelson stellar interferometer, on the left with high visibility. This indicates that the distance between the mirrors was smaller than the coherence length. On the right side the contrast is much lower, indicating that the distance between the mirrors was larger than the coherence length. This effect can be used to accurately determine the coherence length.⁴

The distance for which visibility of the interference pattern is equal to $\frac{1}{e}$. This is the coherence length or the distance beyond which the field has lost phase relation. From this the size of the source can be inferred by using the van Cittert-Zernike theorem, which will be explained in-dept in the next section. Comparable techniques are still used to this day to find the size of stellar objects.

Starlight at the source is spatially incoherent. However the spatial coherence of light increases after propagation as we will see in the next section, making the interferometer successful. The essence of the Michelson stellar interferometer is that a double slit can be used to determine the coherence length or the amount of spatial modes observed. This will be used for the section: Experiment: Spatial fluctuations.

Van Cittert-Zernike theorem

Given a spatially incoherent source of light and enough propagation the result will be spatially coherent light. This effect is described by the van Cittert-Zernike theorem. First the theorem will be stated, including the assumptions that must be true. Thereafter the theorem will be explained qualitatively.

In order for the the van Cittert-Zernike theorem to hold, some conditions must be met. First of all the source must be spatially incoherent. This is true for almost all astronomical sources and thermal sources. The source must be located in the far field and the source emits quasi-monochromatic light. Using a simple filter, this last requirement can be met. Now the van Cittert-Zernike theorem is given by:

$$\Gamma(u, v) = \int \int_{source} I(l, m) \exp(-2i\pi(ul + vm)) dldm \quad (9)$$

⁴Source figure: Photon Engineering, <https://photonengr.com/wp-content/uploads/2017/01/White-light-interference-pattern-768x333.jpg>

This relates the unnormalized spatial coherence function $\Gamma(u, v)$ via a two dimensional Fourier transform to the intensity $I(l, m)$ of the source. l, m are the cosines of the vectors pointing to the source and u, v are the observing plane in units wavelength. (Thompson, Moran, & Swenson, 2017)

But why does spatial coherence increase during propagation? To answer this question, we must recall the concept of spatial modes and spatial coherence. The further an observer is separated from the source, the smaller is the apparent angular size of the source. If the setup remains the same then it is expected that the amount of spatial modes decreases. (Remember: Source size (in unit wavelengths) \cdot solid angle is constant for spatial modes.) This means that the spread of wavevectors that it received is reduced, and thus will the spatial coherence increase. In other words, the source light as a whole does not become more coherent, but you are just selecting a more coherent part of the light. (Born & Wolf, 1980)

So, the reason why spatial coherence increases with distance is because fewer spatial modes are observed from the source. This is quantified in the beautiful van Cittert-Zernike theorem. This provides a way to easily calculate the spatial coherence function given a very simple property of the light source, namely the intensity.

Photons per mode of a thermal light source

Thermal light sources are one of the most abundant and chaotic sources in the universe. The spatial and temporal coherence of a thermal light source are (without filtering) insignificant. However to do experiments with light, the source needs to emit a detectable amount of photons per mode. For a classical thermal source the amount of photons per mode $\mathcal{N}(\omega)$ is neatly described by a Bose-Einstein distribution: (Grynberg et al., 2010)

$$\mathcal{N}(\omega) = \frac{1}{\exp(\hbar\omega/\kappa_B T) - 1} \quad (10)$$

In which \hbar is the reduced Plank constant, ω the angular frequency of the light, κ_B the Boltzmann constant and T the temperature. Filling in this formula for the sun ($T_{eff} = 5800$ K, $\lambda_{peak} = \pm 500$ nm) and looking at the peak frequency ($\omega_{peak} = 3.8 \cdot 10^{15}$ rad/s) leaves us with ~ 0.01 photons per mode.

Using such a low amount of photons per mode will pose a hard experimental challenge. One solution would be to measure with equipment that produces much less noise than the amount of photons per mode. Even then the measurement times will be very long in order to find significant results. The solution chosen for the experiments is to use quasi-thermal light sources. These are light sources that will behave (to some extent) like a thermal light source, but will send out a lot more photons per mode making detection much easier.

Experiment: Spatial fluctuations

The first experiment will involve finding spatial fluctuations for a chaotic light source, which is the same as detecting only a few spatial modes. First the setup will be presented, then a prediction based on theory will be made, after which the experimental results will be shown. The results will be compared to the prediction in the discussion at the end of this section.

A high power LED is chosen as light source. This is a chaotic broad spectrum source. So it can be used to emulate a thermal light source. In order to measure spatial fluctuations, the amount of spatial modes needs to be reduced to only a few. The easiest way to do this, is to use pinholes to spatially filter the light. The setup involves sending the light through two diaphragms. A diaphragm essentially is a pinhole of which the radius is variable. The first diaphragm is used to control the diameter of the light source, and the second diaphragm is to control the size of the observing plane. The light is then send through a double slit, in order to create an interference pattern. The interference pattern is observed by the beam profiler. There are two lenses in this setup. The first is used to collimate the beam and the second is used to image the interference pattern on the beam profiler.

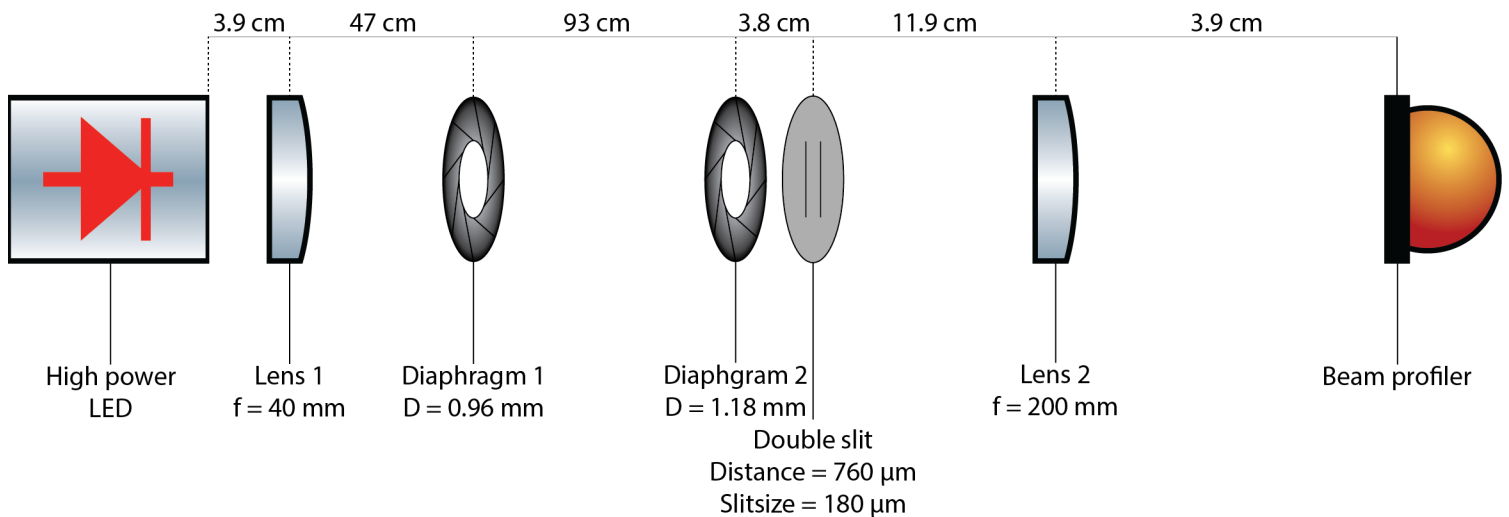


Figure 7: Setup to detect spatial fluctuations. The important properties are written under each component and the distance between each component is written on top. A high power LED is used as light source. The light is collimated by a lens, send through two diaphragms. The first is used to control the size of the light source and the second is used to control the size of the observing plane. A double slit is used to create a spatial interference pattern and finally using another lens the pattern is imaged on the beam profiler. For more details on the setup, see: Appendix A: List of experimental equipment

The high power LED has a frontal power of 1.02 ± 0.01 mW and the peak wavelength is 623 nm. The spectrum is shown in the figure below. We can see that the spectrum is almost symmetric around the peak wavelength. A fact that will be used to make the prediction of the amount of spatial modes the LED sends out.

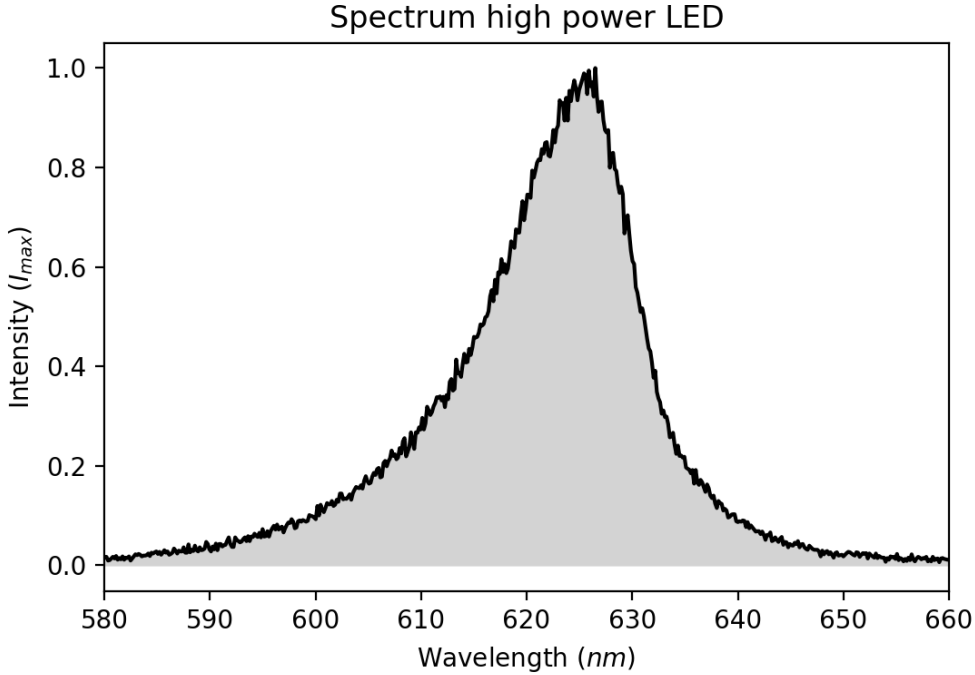


Figure 8: Measured spectrum of the LED used for the spatial fluctuations setup. The spectrum is relative to the maximum spectral intensity. The power in front of the led is 1.02 ± 0.01 mW and the peak wavelength is 623 nm. A feature later used is that the spectrum is almost symmetric around the peak wavelength.

Now we are going to predict what will be observed using this setup.

Prediction

First the amount of spatial modes of the high power LED will be predicted. This can then be used to make a prediction of the power per spatial mode.

The high power LED has a peak wavelength of 623 nm. For the following calculations, the LED will be approximated as a quasi-monochromatic light source of wavelength 623 nm. This makes calculating the exact amount of modes much less complicated. The active element of the LED is measured to be $1 \text{ mm} \cdot 1 \text{ mm}$ (area of the source). Using the diffraction limit for circular sources:

$$\theta = 1.22 \frac{\lambda}{D} = 7.6 \cdot 10^{-4} \text{ rad} \quad (11)$$

This is the angle in radians for one spatial mode. The power of the high power LED is measured over $2\pi \text{ sr}$. The amount of modes that fit in $2\pi \text{ sr}$ are:

$$N_{\text{spatial modes}} = \left(\frac{\pi}{\theta}\right)^2 = 1.7 \cdot 10^7 \quad (12)$$

So in front of the high power LED fit $1.7 \cdot 10^7$ spatial modes. The power measured in front of the same LED is measured to be 1.02 mW. This gives:

$$P_{\text{spatial mode}} = \frac{1.02 \text{ mW}}{1.7 \cdot 10^7} = 0.061 \text{ nW} \quad (13)$$

The prediction is that if the setup detects only a single spatial mode then the corresponding detected power will be: $P_{\text{spatial mode, predicted}} = 0.061 \text{ nW}$.

Results

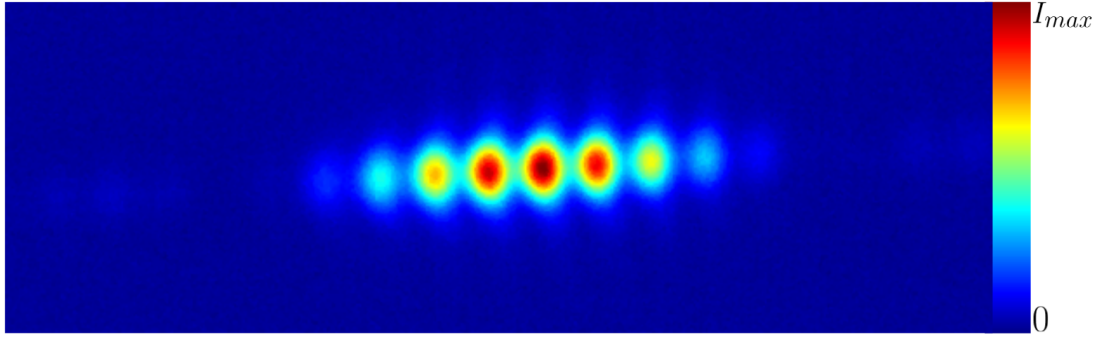


Figure 9: Interference pattern as measured by the beam profiler. The minimum value in between the peaks is $0.5I_{\text{max}}$. The total power of the interference pattern corresponds to $P_{\text{measured}} = 0.062 \text{ nW}$

The interference pattern observed by the setup is given in the figure above. Clearly visible are the different fringes, so even though the LED sends out spatially incoherent light, it is possible to observe fluctuations. The minimum intensity in the interference pattern is half of the maximum intensity. The resulting spatial coherence is (see eq. 5):

$$\Gamma_{\text{Interference pattern}} \approx \frac{1}{3}$$

The total power of the interference pattern corresponds to:

$$P_{\text{measured}} = 0.062 \text{ nW}$$

Discussion

There is a small oversight in the setup. The distance between the slits is smaller than the diameter of the second diaphragm. The second diaphragm is not the limiting factor of the observing plane. In other words the second diaphragm is probably unnecessary in the setup.

There are multiple measurement errors and approximations which will cause the prediction to be only accurate to an order of magnitude. First of all the size of the active element was very hard to accurately measure, as the active element of the LED is covered in a plastic lens. The measurement was done by eye, so the $1 \text{ mm} \cdot 1 \text{ mm}$ can easily be off by twenty percent.

The output power of the LED was measured by simply putting a power meter in front of it. It could have been that not all the light in front of the LED has been collected. However the lens in front of the led should focus most light to the front of the LED, but still this introduces an error.

Also the LED was assumed to be a quasi-monochromatic light source which only sends light at its peak wavelength ($\lambda_{\text{peak}} = 623 \text{ nm}$). This was based on the fact that the spectrum of the LED is almost symmetric for this wavelength. (See figure 8 for the spectrum.) However this is an approximation of the real situation and so introduces errors.

Lastly, the spatial coherence of the of the resulting interference pattern is $\Gamma_{\text{measured}} = \frac{1}{3}$. This means that the interference pattern is the result of more than one spatial mode. So P_{measured} should be divided by an unknown amount of $N_{\text{spatial modes}} > 1$ to get the measured power per spatial mode.

Comparing the predicted power per mode based on theory to the power measured of the interference pattern, we see that there is only a very small difference.

$$P_{\text{spatial mode, predicted}} = 0.061 \text{ nW}$$

$$P_{\text{measured}} = 0.062 \text{ nW}$$

The difference between these values is 0.001nW, which is most probably a coincidence. Based on the reasons stated above, it would be expected that the difference between the values will be in the order of a magnitude instead.

Either way, it should be clear that a simple setup involving two pinholes is already sufficient to filter only a few spatial modes, as we can observe interference and the power measured of the interference pattern is almost the same as the power predicted for a single spatial mode.

Second order correlation function

Observing temporal fluctuations in chaotic visible light is a big experimental challenge. Due to the very broad bandwidth of most thermal light sources (already around 10 THz for the earlier mentioned high power LED) is the direct observation of temporal fluctuations impossible. Even very fast cameras go up to about a \sim MHz in shutter speed. So in order to get a factor 1000 closer to the frequency of light, single photon detectors will be used. These have a 'shutter speed' of about \sim GHz, however single photon detectors only observe intensity. So direct observation of the electric or magnetic field is not possible. To still find out whether a single temporal mode is observed, we can study the second order correlation function $g^{(2)}$. (Mandel & Wolf, 1995)

The second order correlation function is defined as:

$$g^{(2)}(\tau) = \frac{\langle I(t)I(t+\tau) \rangle}{\langle I(t) \rangle^2} \quad (14)$$

The function correlates the intensity measured at certain time t with the intensity at delayed time $t + \tau$. This is then divided by the square of the intensity in order to normalize the function. The angle brackets denote an ensemble average. For coherent light (such most lasers) this function will return a value of 1. However for thermal light this is not always the case, as we will see in the next section.

Correlation of thermal light

For most values of τ of thermal light the second order correlation function will be 1. However if the time delay goes to zero, the value of $g^{(2)}$ goes up to two. This effect will now be explained. Thermal light has some curious properties. One of them being that the variance of the intensity is given by:

$$var(I) = \bar{I} + \frac{\bar{I}^2}{N_{\text{modes}}} \quad (15)$$

With \bar{I} being the average intensity detected and N_{modes} is the amount of modes detected. Based on Poisson statistics it is expected that the variance of the intensity is equal to the average intensity, however the second term is specific for thermal light. This term goes to zero if many modes are detected. If one spatial mode is observed then for $g^{(2)}(\tau = 0)$ only one spatial-temporal mode is observed. This gives the following variance:

$$var(I) = \bar{I} + \bar{I}^2 \approx \bar{I}^2 \quad (16)$$

The last approximation assumes high intensity. The deviation of the intensity is then given by:

$$\sqrt{var(I)} = \Delta I \quad (17)$$

The Δ is used to note that deviation of the photon numbers or intensity can be positive just as well being negative. Now define the intensity as:

$$I(t) = \bar{I} + \Delta I \quad (18)$$

The bar denoting the average intensity. Putting the intensity of a single mode into the $g^{(2)}(0)$ gives:

$$g^{(2)}(0) = \frac{\langle I(t)I(t) \rangle}{\langle I(t) \rangle^2} = \frac{\langle \bar{I}^2 + \Delta I^2 + 2\bar{I}\Delta I \rangle}{\langle \bar{I} + \Delta I \rangle^2} = \frac{\bar{I}^2 + \Delta I^2}{\bar{I}^2} = \frac{2\bar{I}^2}{\bar{I}^2} = 2 \quad (19)$$

After taking the ensemble average, all the terms with only a single ΔI average to zero. Realize in the second to last step, that $\Delta I^2 = var(I) = \bar{I}^2$. (Fox, 2006) For thermal light the $g^{(2)}(0)$ is expected

to peak to values as high as 2 if only a single temporal modes is detected. So experimentally finding a value of the second order correlation function higher than one, is the same as detecting only a few modes. Detecting only a few modes must give fluctuations. Experiment: Temporal fluctuations revolves around this reasoning.

Fabry-Pérot filter

Using the second order correlation function, single photon detectors can be used, which can measure fluctuations happening at frequencies in the GHz regime, however fluctuations in unfiltered thermal light happen a million times faster, which can be inferred from invariant product for temporal modes (see table 1):

$$\Delta\nu \cdot \Delta t = 0.44 \quad (20)$$

Here, $\Delta\nu$ is the spectral width of the source in Hz and Δt is the fluctuation timescale time. This product is exactly equal to 0.44 for a Gaussian shaped spectrum.

The last missing piece of the puzzle for detecting temporal fluctuations is very narrow filtering of the light. This will be done using a Fabry-Pérot filter.

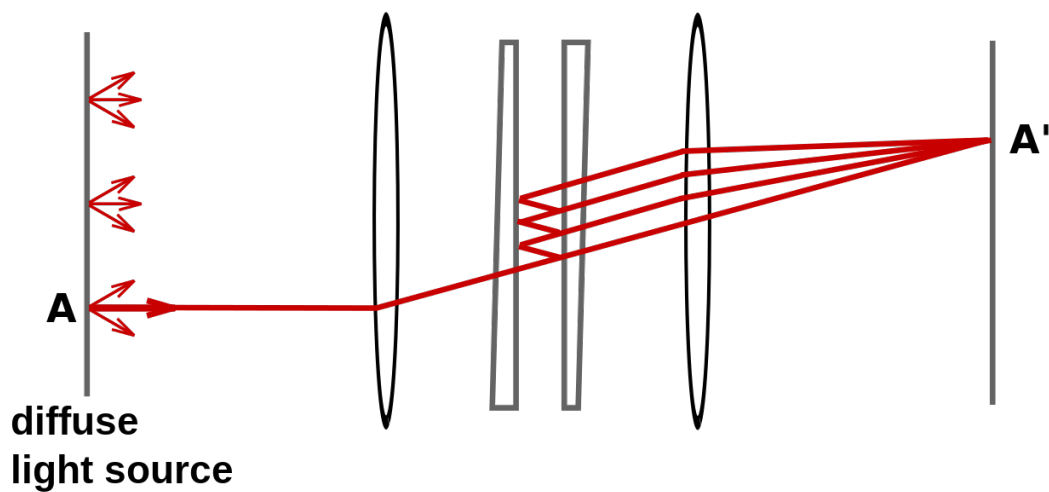


Figure 10: Schematic of a Fabry-Pérot cavity. In the middle are two mirrors. In between these mirrors the light starts to interfere with itself. This results in only certain wavelengths passing through, while others are blocked. The lenses are only used for focusing the light.⁵

A Fabry-Pérot cavity works in the following way. Two mirrors are put close together, creating a cavity. Light sent into this cavity starts to bounce back and forth between the mirrors. This creates a resonating cavity, which for certain wavelengths is reflective, while other wavelengths can easily pass through the cavity. A transmission spectrum with multiple evenly spaced peaks is created.

⁵By Stigmatella aurantiaca - Own work, CC BY-SA 3.0

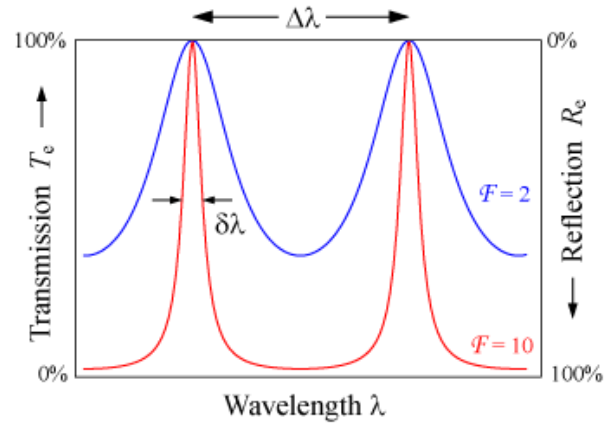


Figure 11: Spectrum after two different Fabry-Pérot cavities. $\Delta\lambda$ is the free spectral range. $\delta\lambda$ is the full width half max (FWHM) of the peak. In red is a cavity with higher finesse. It results in narrower peaks than the cavity with lower finesse (the blue line).⁶

The spacing between the peaks is called the free spectral range (FSR). The free spectral range in frequency is given by:

$$\Delta\nu_{\text{FSR}} = \frac{c}{2L} \quad (21)$$

c is the speed of light and L is the distance between the mirrors. The finesse and full width half max (FWHM) given in frequency of the peaks are given by:

$$\mathcal{F} = \frac{2\pi}{-\ln(R^2)} \quad (22)$$

$$\Delta\nu_c = \frac{\Delta\nu_{\text{FSR}}}{\mathcal{F}} \quad (23)$$

Here, R is the reflectivity of the mirrors used for the cavity. To use successfully a Fabry-Pérot cavity as a filter, the free spectral range must be large in order to ensure that only a single (or a few) are measured after the cavity. On the other hand the Finesse must be high in order to ensure that the FWHM of the peaks is in line with the desired filtering.

⁶By English Wikipedia user DrBob, CC BY-SA 3.0, <https://commons.wikimedia.org/w/index.php?curid=6409024>

Experiment: Temporal fluctuations

By measuring the second order correlation function, temporal fluctuations can be found. If the second order correlation function shows a peak then only a few temporal modes are observed, which indicates fluctuations. (See: Correlation of thermal light) First the setup used for the measurement of the second order correlation function will be presented, then a numeric simulation of the expected results will be presented, after which the results of the experiment will be presented. In the end, the results will be discussed.

To measure temporal fluctuations a superluminescent LED (SLED) is chosen. This is laser-like light source, but it is still temporally incoherent. Using a SLED had two advantages. The first being that the output is coupled to a single mode fiber. All the light will be send in one spatial mode. The second advantage is that the amount of photons per mode is very large (~ 1000).

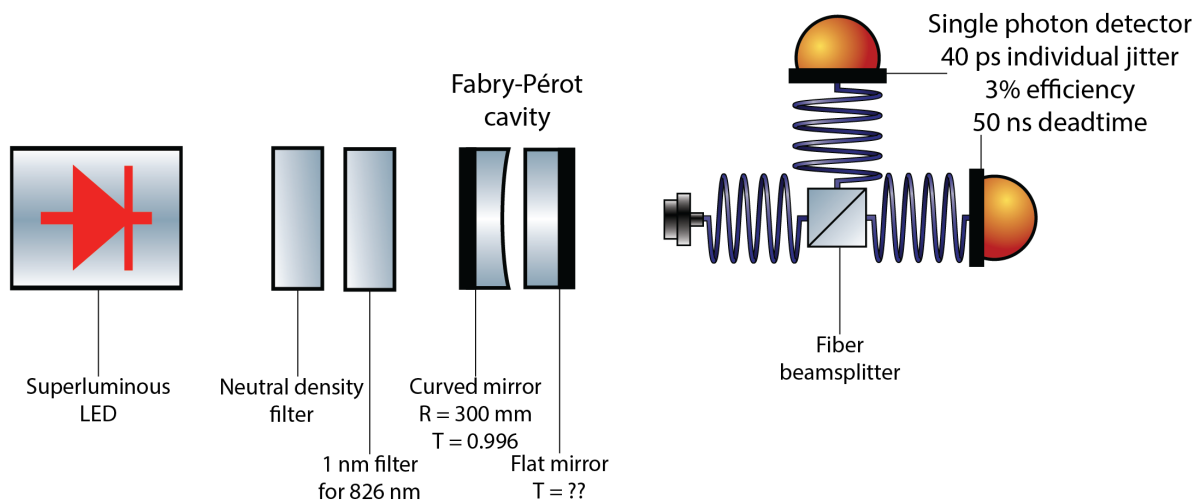


Figure 12: Setup for measuring temporal fluctuations. The light source is a super luminescent LED. This is a single mode coupled light source with a very low temporal coherence. The light is then passed through a neutral density filter in order to reduce the intensity. Then it passes through a spectrum filter. To filter the light further a Fabry-Pérot cavity is used, which consists of a curved and a flat mirror. (R is the radius of curvature and T is the transmission.) The resulting light is coupled into a multi mode fiber, which is then split to do a second order correlation measurement with two single photon detectors. The detectors have a combined jitter time of 50 ps (Snijders et al., 2018). See: Appendix A: List of experimental equipment for the exact equipment used.

Taking a look at the setup, we find that the temporal resolution is limited by the jitter time of the detectors. The individual single photon detectors can detect the arrival time of photons with an accuracy of 40 ps, however the combined jitter time is a bit higher: 50 ps. So the coherence time should be about the same in order to observe a peak. The coherence time can be found using the invariant product for temporal modes (see table 1):

$$\Delta\nu \cdot \Delta t = 0.44 \quad (24)$$

$\Delta\nu$ is the spectral width in Hz and Δt is the coherence time (or fluctuation timescale). This is exactly equal to 0.44 for a Gaussian spectrum. In short the coherence time is inversely proportional with the spectral width.

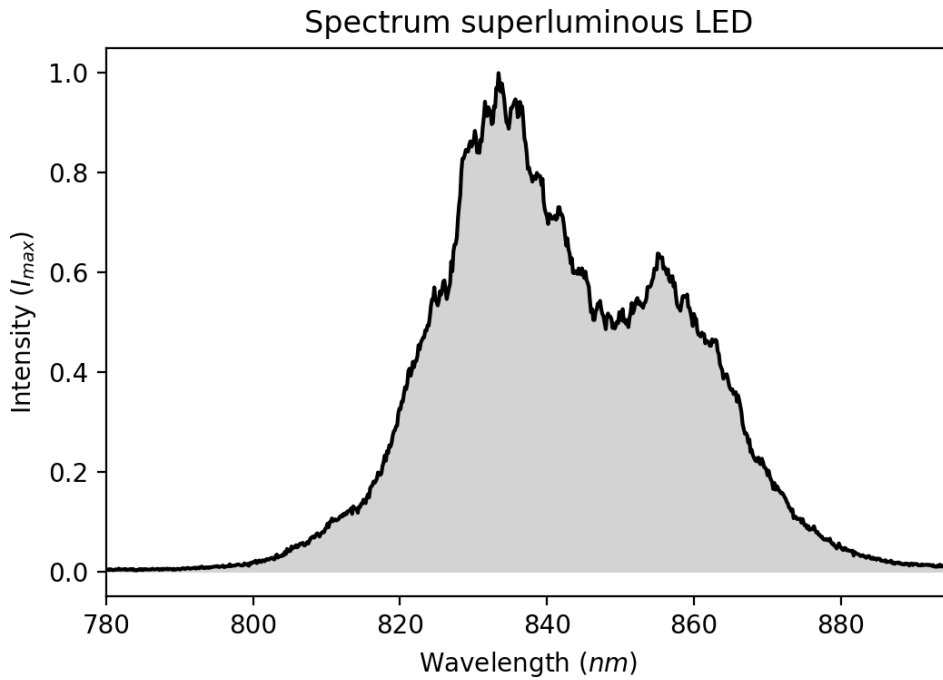


Figure 13: The spectrum of the superluminescent LED (SLED) scaled to the maximum intensity. The coherence time of the spectrum is $4 \cdot 10^{-14}$ s

Measuring the spectrum of the SLED (and using eq. 24) gives us a coherence time of $4 \cdot 10^{-14}$ s. This is much shorter than the combined jitter time of the detectors, so a 1 nm filter is used.

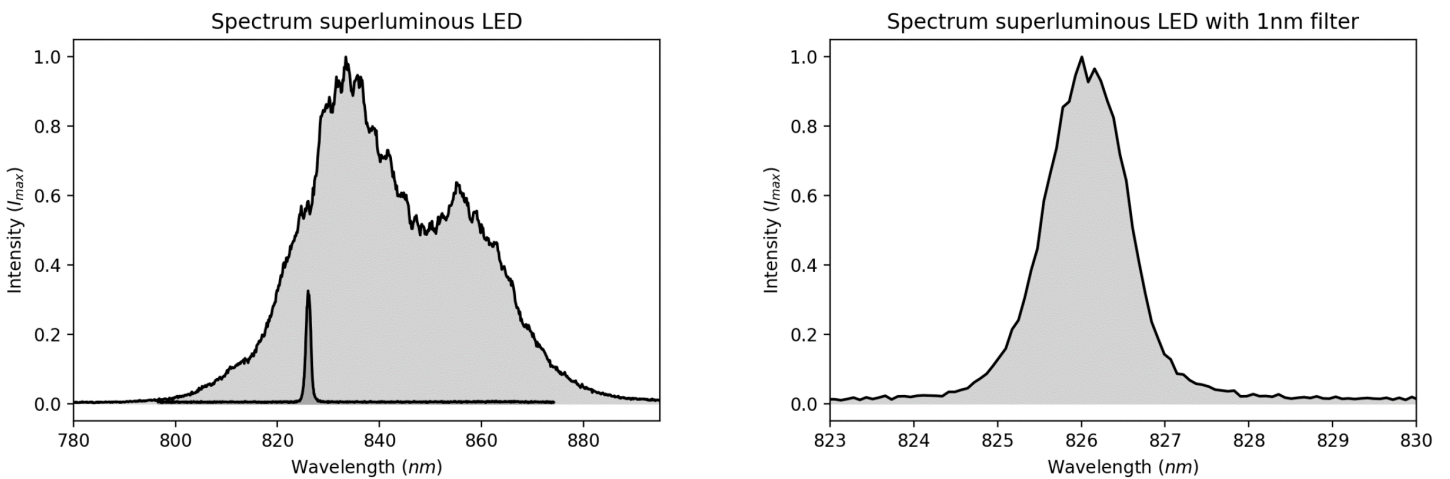


Figure 14: The left shows the spectrum of the SLED in light gray and the spectrum of the SLED after the filter in dark gray. Both are scaled to the maximum intensity of the SLED. A rescaled zoom-in of the filtered spectrum is shown on the right. This results in a coherence time of $2 \cdot 10^{-12}$ s.

The 1 nm filter increases the coherence time by two orders, however it is still far too short. In order to increase the coherence time even further the Fabry-Pérot filter is used. The goal is to build a Fabry-Pérot cavity that has a free spectral range that is larger than 1 nm, so only one peak is expected after the cavity. Also the FWHM of the peak should be 0.03 nm in order to reach a coherence time of 100 ps. A coherence time of 100 ps assures that at least two data points fall inside the same mode. So a peak in the second order correlation function should be visible.

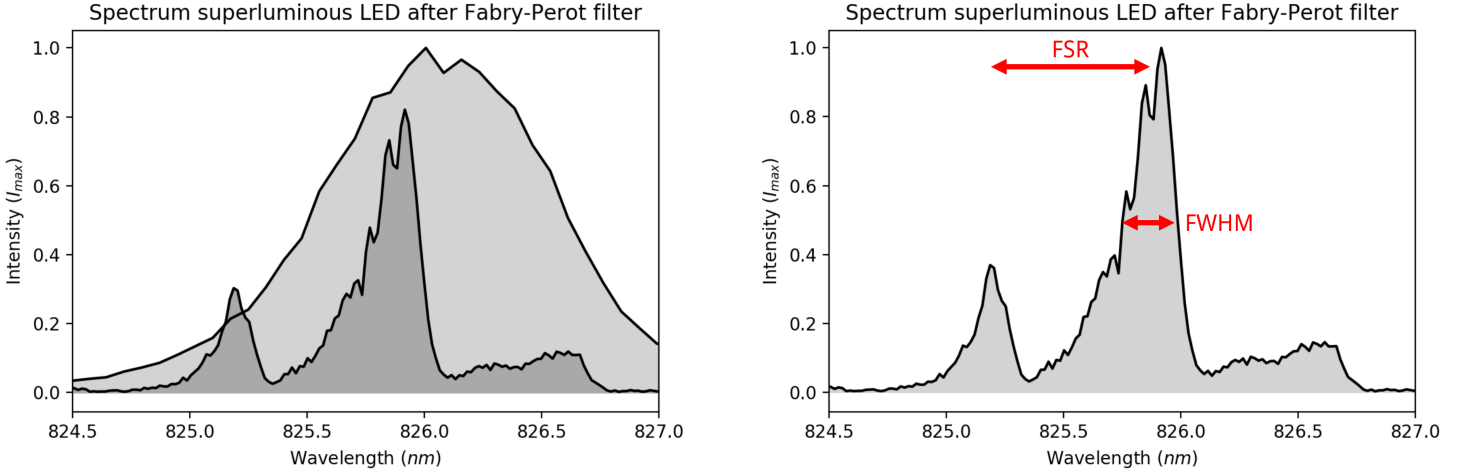


Figure 15: The left shows the spectrum of the SLED after the 1 nm filter in light gray and the spectrum of the SLED after Fabry-Pérot filter in dark gray. The spectra do not overlap perfectly, because a different spectrum meter was used for the Fabry-Pérot spectrum. This introduced an offset. A rescaled zoom-in of the Fabry-Pérot spectrum is shown on the right. The free spectral range and FWHM of the peaks are shown. The FSR corresponds to 0.8 nm and the FWHM to 0.3 nm. This results in a coherence time for the central peak of $1 \cdot 10^{-12}$ s.

The Fabry-Pérot filter nearly reaches the intended goals.

$$FSR_{\text{goal}} = 1 \text{ nm}, FSR_{\text{real}} = 0.8 \text{ nm}$$

$$FWHM_{\text{goal}} = 0.03 \text{ nm}, FWHM_{\text{real}} = 0.3 \text{ nm}$$

The free spectral range only falls a bit short of the intended goal. This will not be a problem, as the introduced side peaks are still much lower than the central peak. However the FWHM of the central peak is a factor 10 broader than intended. This will make the combined jitter time of the detectors a factor 50 larger than the coherence time.

To investigate what the effects of the filter will be a simulation is made.

Numeric simulation

In order to predict the results of the second order correlation function ($g^{(2)}$) for the previously described setup, a numerical simulation of the correlation of thermal light is made. First a proof of concept of the simulation will be shown, then the simulation will conceptually be explained. Finally, the simulation will be run with values in line with the experimental situation as to predict the $g^{(2)}$. The simulation should clearly show two things. The first being a peak for $g^{(2)}(\tau = 0)$. The second being the effect of coherence time.

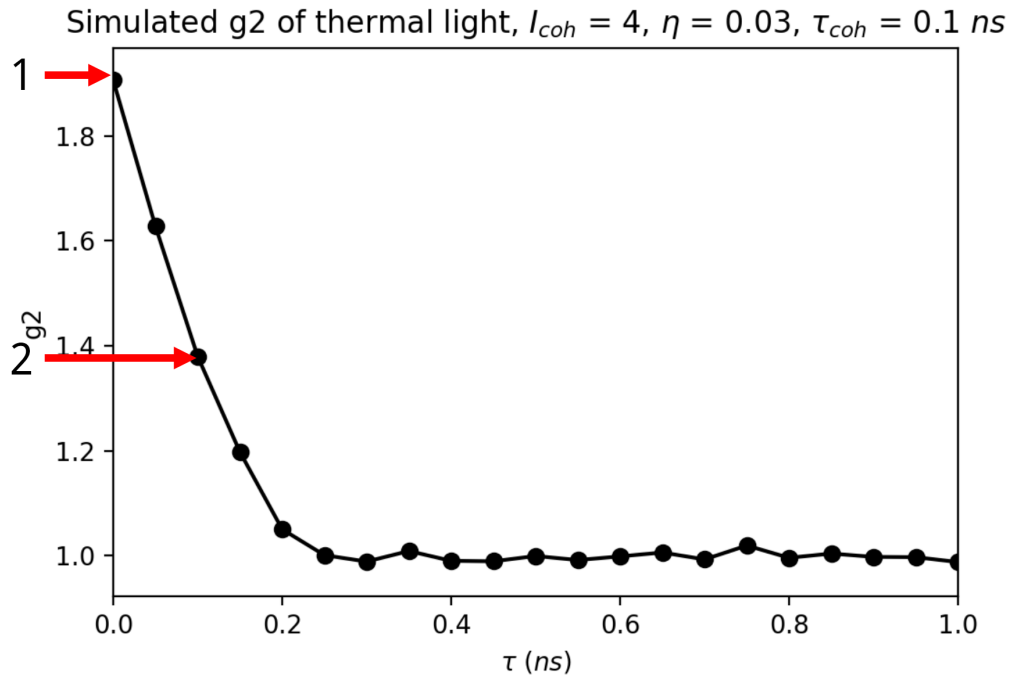


Figure 16: Proof of concept of the simulation of the second order correlation function of thermal light. The circles are the simulated data points. A line is drawn between these points. This run has an average intensity of 4 photons per coherence time. A detector efficiency of 3% is assumed, which matches the efficiency of the real detectors, and a simulated coherence time of 100 ps. Marked with a 1 is the peak $g^{(2)}(0)$, which is expected for thermal light. Marked with a 2 is the effect of the coherence time, without accounting for the effect of detector jitter.

The simulation correctly shows the peak for $g^{(2)}(0)$ which is expected for thermal light. The decay in the second order correlation also works like it is expected to. After one coherence time, $g^{(2)}$ is at half the peak value. The above simulation is done with a coherence time of 100 ps. The simulation of thermal light will now be conceptually explained.



Figure 17: First an intensity stream is created. This is done by randomly switching the intensity between 0 and $2I$ for N times. $N = 1000$ for the simulations shown.

First an intensity stream is created. This stream must have an average intensity of I and a variance of I , because this is expected for thermal light. By switching between $2I$ and 0 this variance and average is reached.

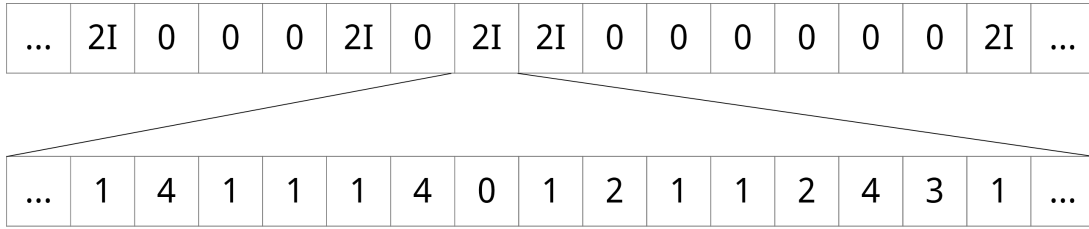


Figure 18: Next each of the intensities simulated will be used to seed streams of a uniformly chosen length between 0 and $3\tau_c$. These streams are filled with samples from a coherent (Poisson) distribution. In the above example: $I = 1$.

The coherence time is simulated by expanding each of the intensity values of the intensity streams into a coherent photon stream of a length uniformly chosen between zero and three times the coherence time. This results in the simulation of the coherence time.

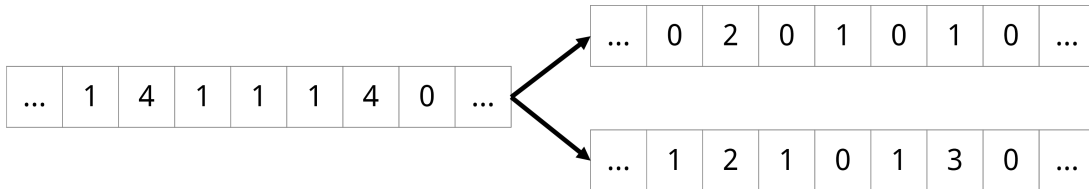


Figure 19: The photon stream is split in two photon streams, by using a binomial distribution. This simulates the beam splitter.

Next the beam splitter is simulated. The photon stream is divided in two evenly distributed photon streams using a binomial distribution.



Figure 20: Each of the photon streams are converted to detection events. The result is that the efficiency of the detectors are simulated.

The photon numbers are then converted to detection events. The chance for a detection event is:

$$P(\star) = 1 - (1 - \eta)^n \tag{25}$$

With η being the detection efficiency and n the incoming photons.

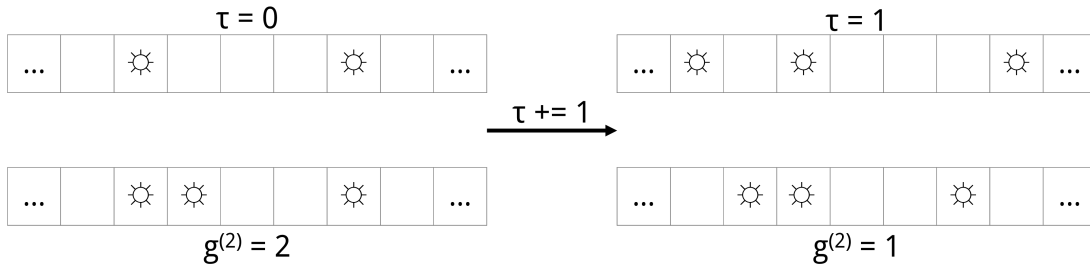


Figure 21: The correlations are calculated by multiplying the two photon streams with each other, summing the resulting correlation events and then shifting the first stream by one time step. This process is repeated for all times τ .

The last step is to calculate the amount of correlations for each delay τ . This is done by multiplying the two photon streams and then shifting the first by one time step. Divide the by the average correlations and the result will be a normalized $g^{(2)}(\tau)$ function. Depending on the input photon stream this method of simulation is also able to simulate the $g^{(2)}(\tau)$ of coherent light and anti-bunched light. See: Appendix B: Second order correlation function simulation code for the code used for the simulation, which includes functions for generating three different kinds of photon streams.

So the simulation works and the workings have been revealed. Let us now take a look at the expectation of the $g^{(2)}(\tau)$ of the experiment based upon the simulation.

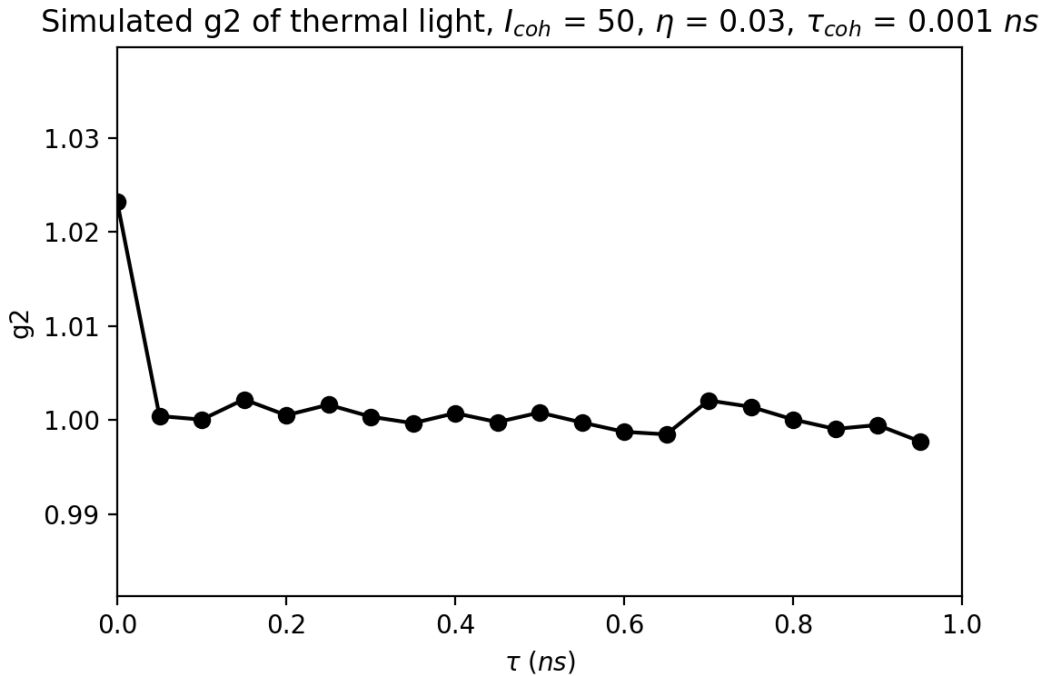


Figure 22: Simulation run with realistic parameters. The intensity per coherence time/mode is 50. The efficiency is set to match the detectors at 3%. The coherence time is set to 1 ps, as is expected based on the central peak of the Fabry-Pérot filtered spectrum.

Based on the simulation the peak of the second order correlation function could be as high as:

$$g^{(2)}(0) = 1.02$$

Experimental results

An experimental challenge not yet discussed is the fact that it is not known where $\tau = 0$ will be for the correlation experiment. Delays can be caused by the length of the optical fibers used and by the electronic components used. The theoretical $\tau = 0$ is therefore not at $\tau = 0$ for the measurement data. The coincidence measurement (see: Fig. 12) is started for 40000 s (~ 11 hours). After the runtime the following results are acquired:

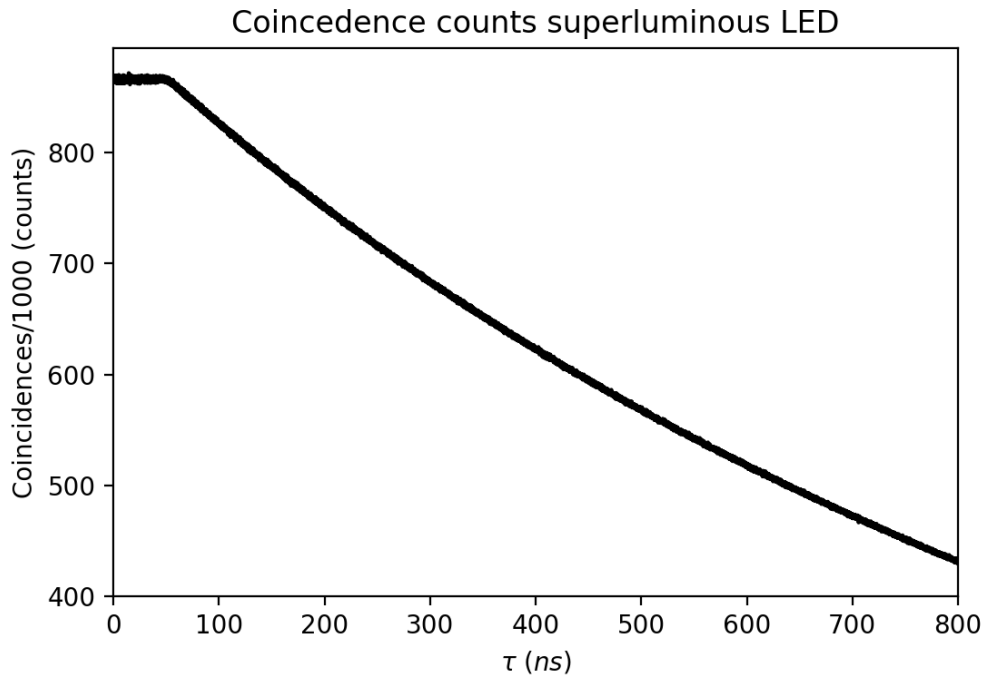


Figure 23: Measured coincidence counts after 40000 s of measuring time. (See: Fig. 12) At about 50 ns the counts start to decay exponentially. This is caused by pile-up effects of the time-correlated single photon counting technique.

The resulting coincidence counts clearly show two regions. In the first 50 ns the amount of counts remain nearly equal, but after 50 ns the amount of counts start to exponentially decay. This is caused by the so called pile-up effect of the time-correlated single photon counting technique. The detectors, being single photon detectors, can only count one photon at a time, after which a dead time (50 ns) occurs. In this dead time no counts can be recorded. The chance that a detection event has occurred, which triggers the dead time increases with the delay time. The effect is that the chance to record a coincidence count starts to decrease after the dead time, which is called the pile-up effect.

Pile-up effects are however not the focus of this research, so now we will take a closer look at the 'flat' region of the coincidence counts.

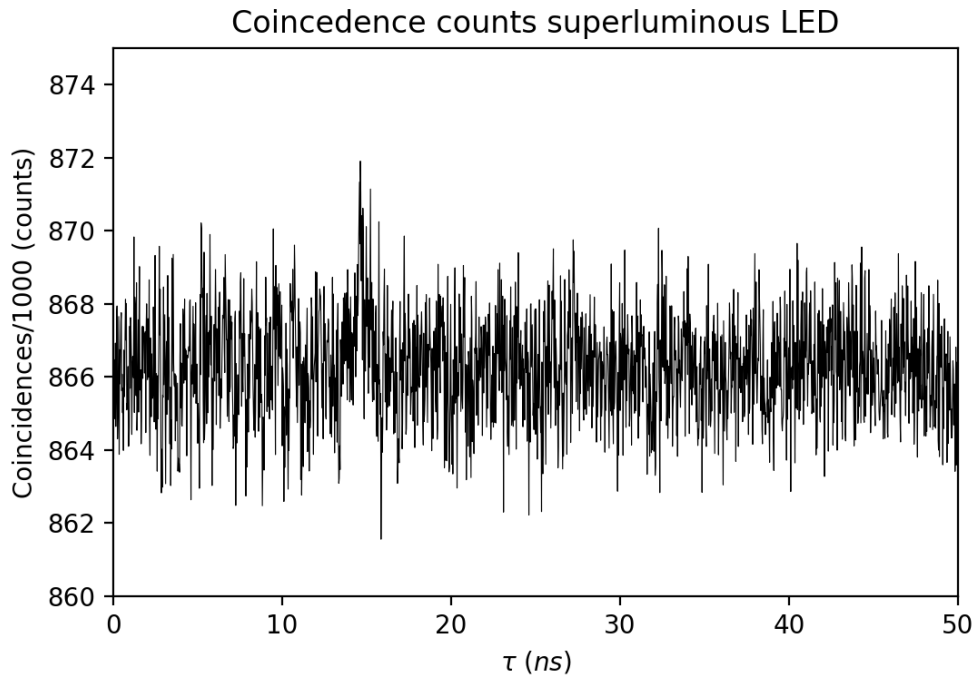


Figure 24: Zoom-in of figure 23. It is unknown where the theoretical $\tau = 0$ is located exactly. A possibly significant peak is found at $\tau = \pm 15$ ns.

A zoom-in of the flat region of the coincidence counts reveals a possible significant peak. This could be the peak that is expected for thermal light at the theoretical $\tau = 0$.

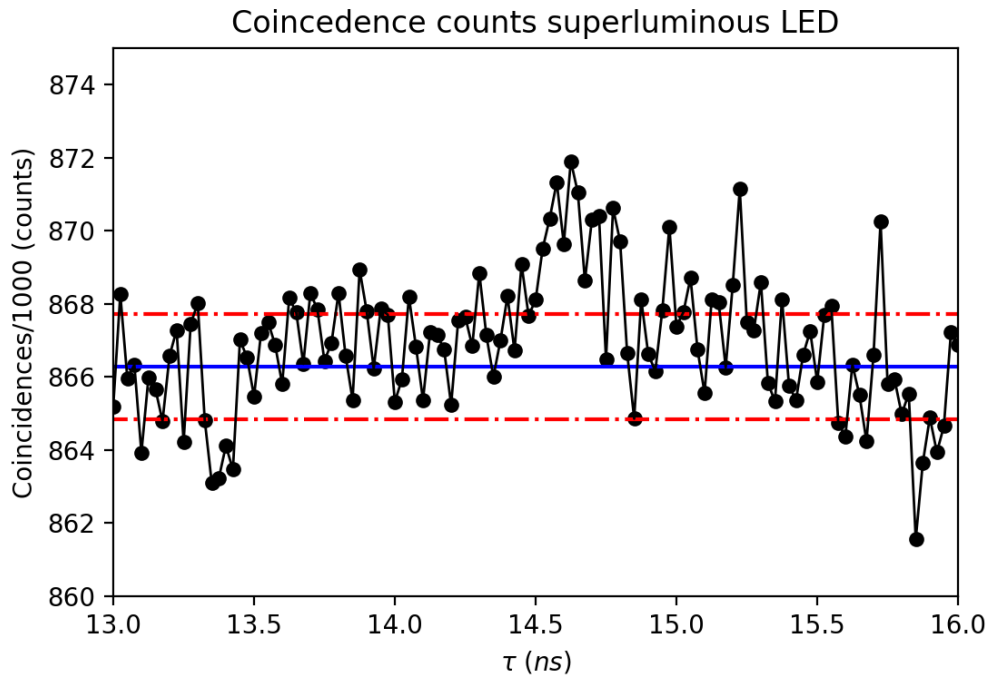


Figure 25: A very close look at the data points around $\tau = 15$ ns. The blue line is the mean value of the whole 'flat' region. (See: Fig. 24) The red dashed line is represents a deviation of one sigma. The peak value in this region corresponds to a significance of 3.9σ .

Taking a even closer look at the region around $\tau = 15$ ns, we see that the peak has a significance of 3.9σ . This means that the chance that the peak is simply a measurement error is around 1 in 10000. However there are also 10000 data points between 0 and 50 ns. Based on these facts, we can assume that the peak is insignificant, however to be sure the measurement is repeated.

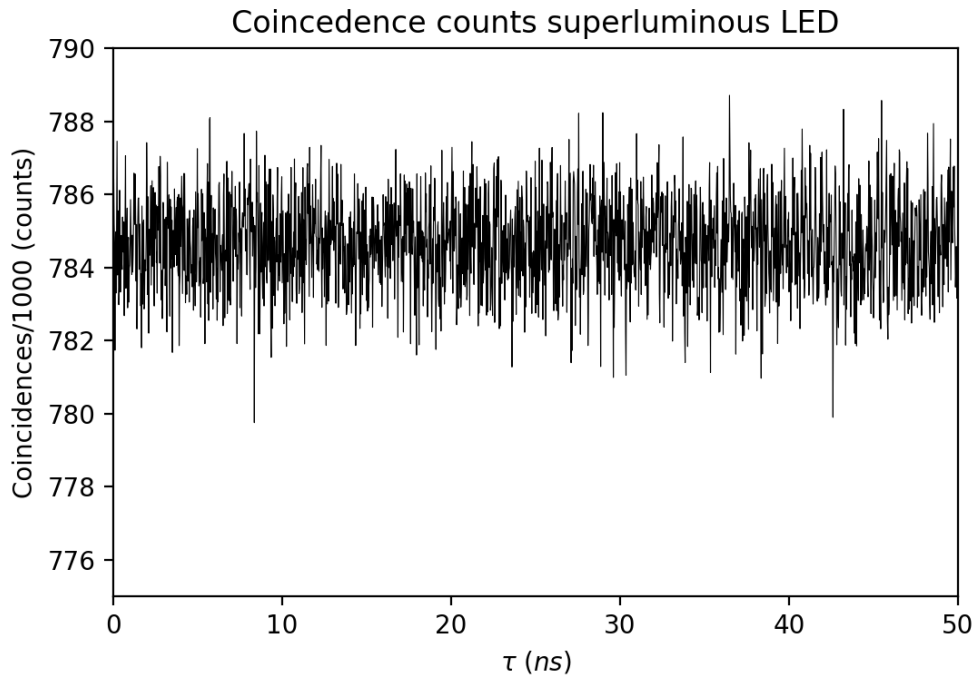


Figure 26: Zoom-in of the second correlation measurement. The runtime is again 40000 s. This time, no clear peak is visible.

Repeating the experiment with the same parameters, does not reveal a peak. In other words no significant results have been found.

Discussion

Simulations based on the setup predicted a peak of $g^{(2)}(0) = 1.02$, however measurements did not reveal a significant peak. If the predictions are correct then the peak should have been found, because the accuracy of the normalized $g^{(2)}$ function of the measurements is around ~ 0.001 .

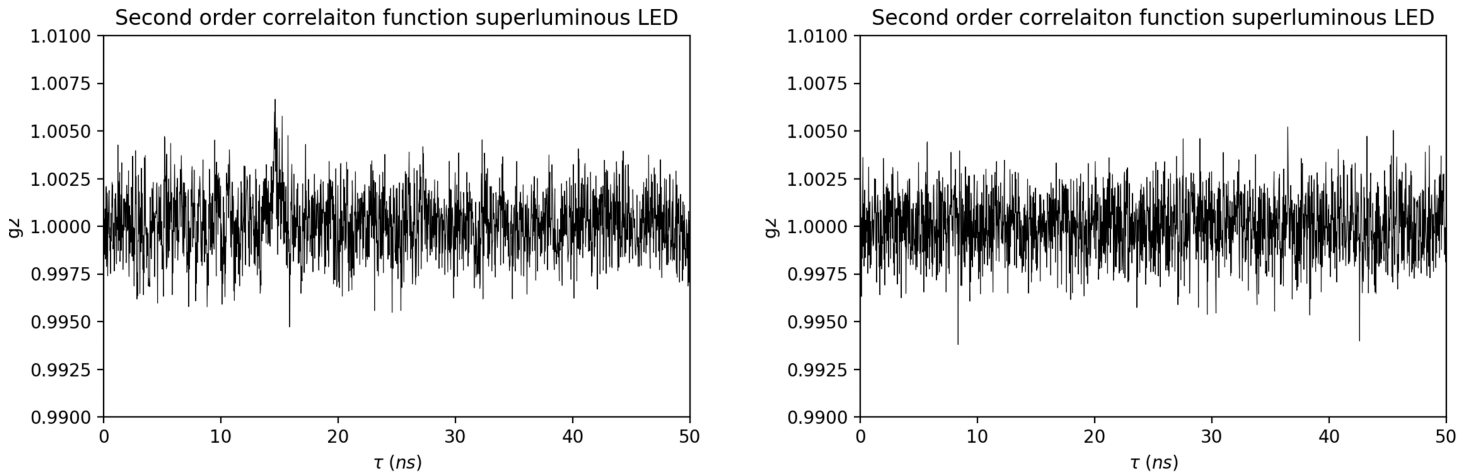


Figure 27: Zoom-ins of the correlation measurements side by side. On the left is the first run and on the right the second. This time the counts are normalized. This reveals an accuracy on the second order correlation function of ~ 0.001 .

The absence of the peak can be explained in one of three ways. First of all, the most obvious. The fluctuations do not exactly behave as is expected for a thermal light source. A superluminescent led was used as a quasi-thermal light source, which should have a very low temporal coherence, so it should behave like a thermal source. However even a very low temporal coherence could cause a decrease in the effect on the second order correlation function. Second, the fluctuations are happening, but they are happening on a much faster time scale than is possible to measure. The simulation did not take the side lobes of the real spectrum in account (See: Fig. 15). This causes an even shorter coherence time than simulated. So the peak value of the second order correlation function will be lower than the simulated value. Third and last, there are experimental limitations. In reality there is of course always some background light, also decreasing the height of the peak in the second order correlation function.

One of these three, or a combination of the reasons listed above can most probably explain the absence of significant effects in the second order correlation function of the filtered superluminescent LED spectrum. A next step would be to improve the performance of the filters and remeasure the data. Also the simulation can be expanded in order to accommodate for the side lobes and background light. This could be used to either find the peak or to better explain the absence thereof.

Conclusion

At the start of the research the following question was proposed: 'Can fluctuations be found in visible thermal light?' For spatial fluctuations the answer is yes. Based on theory, a setup of two pinholes was used for finding spatial fluctuations. Using a high power LED as light source, a double slit was used to image an interference pattern. This interference pattern is clear proof for spatial fluctuations in visible thermal light.

Then an experiment was proposed to measure temporal fluctuations in visible thermal light. The setup consisted of a superluminous led which was filtered in two steps. A second order correlation measurement was conducted with single photon detectors. In theory, the second order correlation function for thermal light should give a peak value of 2 for temporal fluctuations. The setup however did not find any significant results and so the research question remains partly unsolved by the experiments performed in this research.

Whilst the absence of the expected effect for the second order correlation function measurement is unfortunate, a basis has been laid for further theoretical and experimental investigations of fluctuations in visible thermal light. Especially the simulations done are interesting, because with a moderate amount of code and a few approximations, a physically complex process, such as second order correlation of light can be described quite well. Similar simulations have been investigated in recently published researches. (Schneider, Biernoth, Hölzl, Pscherer, & von Zanthier, 2018) (Facão, Lopes, Silva, & Silva, 2011)

We hope that in the future the basis laid in this research will be used to do a in-dept research of the fluctuations of the (in our opinion) most interesting visible thermal light source: The sun.

References

- Born, M., & Wolf, E. (1980). Calculation of mutual intensity and degree of coherence for light from an extended incoherent quasi-monochromatic source. In *Principles of optics: electromagnetic theory of propagation, interference and diffraction of light* (6th, corre ed., pp. 508–516). Oxford: Pergamon Press.
- Brooker, G. (2003). Coherence : qualitative. In *Modern classical optics* (pp. 194–218). Oxford: Oxford University Press USA - OSO.
- Daendliker, R. (2000). Concept of modes in optics and photonics. In J. J. Sanchez-Mondragon (Ed.), *Sixth international conference on education and training in optics and photonics* (Vol. 3831, pp. 193–198). SPIE. Retrieved from <https://doi.org/10.1117/12.388718> doi: 10.1117/12.388718
- Facão, M., Lopes, A., Silva, A. L., & Silva, P. (2011). Computer simulation for calculating the second-order correlation function of classical and quantum light. *European Journal of Physics*, 32(4), 925–934. Retrieved from <https://doi.org/10.1088/0143-0807/32/4/007> doi: 10.1088/0143-0807/32/4/007
- Fox, M. (2006). Photon statistics & Photon antibunching. In *Quantum optics: an introduction* (pp. 75–117). Oxford: OUP Oxford.
- Grynberg, G., Aspect, F., & Alain, C. (2010). Complement 3C: Laser light and incoherent light: energy density and number of photons per mode. In A. Aspect, C. Fabre, & G. Grynberg (Eds.), *Introduction to quantum optics: From the semi-classical approach to quantized light* (pp. 277–287). Cambridge: Cambridge University Press. Retrieved from <https://www.cambridge.org/core/books/introduction-to-quantum-optics/complement-3c-laser-light-and-incoherent-light-energy-density-and-number-of-photons-per-mode/DDC084BDB02DDD3DEA8C63919198ADA8> doi: DOI:10.1017/CBO9780511778261.015
- Mandel, L., & Wolf, E. (1995, sep). Radiation from sources of any state of coherence. In *Optical coherence and quantum optics* (pp. 229–337). Cambridge: Cambridge University Press. Retrieved from <https://www.cambridge.org/core/product/identifier/9781139644105/type/book> doi: 10.1017/CBO9781139644105
- Michelson, A. A., & Pease, F. G. (1921). Measurement of the diameter of Alpha-Orionis by the interferometer. *Proceedings of the National Academy of Sciences of the United States of America*, 7(5), 143.
- Schneider, R., Biernoth, C., Hölzl, J., Pscherer, A., & von Zanthier, J. (2018, aug). Simulating the photon stream of a real thermal light source. *Appl. Opt.*, 57(24), 7076–7080. Retrieved from <http://ao.osa.org/abstract.cfm?URI=ao-57-24-7076> doi: 10.1364/AO.57.007076
- Snijders, H., Frey, J. A., Norman, J., Post, V. P., Gossard, A. C., Bowers, J. E., ... Bouwmeester, D. (2018). Supplemental Material: Fiber-Coupled Cavity-QED Source of Identical Single Photons. *Phys. Rev. Applied*, 9(3). Retrieved from <https://link.aps.org/doi/10.1103/PhysRevApplied.9.031002> doi: 10.1103/PhysRevApplied.9.031002
- Thompson, A. R., Moran, J. M., & Swenson, G. W. (2017). Van Cittert-Zernike Theorem, Spatial Coherence, and Scattering. In *Interferometry and synthesis in radio astronomy* (pp. 767–786). Cham: Springer International Publishing. Retrieved from <http://link.springer.com/10.1007/978-3-319-44431-4> doi: 10.1007/978-3-319-44431-4

Appendix A: List of experimental equipment

Experiment: Spatial fluctuations

- Spectrometer: Triax 550 (300, 600, 1200 lines/mm)
- Power source: Thorlabs LDC 205 B laser diode controller
- Beam profiler: Cinogy cincam cmos 1201 nano

Experiment: Spatial fluctuations

- Spectrometer: Triax 550 (300, 600, 1200 lines/mm)
- Spectrometer (Fabry-Pérot spectrum): FHR 1000
- Power source: Thorlabs LDC 205 B laser diode controller
- Light source: Thorlabs sled LM14S2
- Single photon detector: ID Quantique ID 100 MMF50
- Correlation card: TimeHarp 260 PICO
- Beam splitter: Thorlabs TM105R5F1B

Appendix B: Second order correlation function simulation code

```
from numpy import *
import numpy as np
from matplotlib.pyplot import *
import matplotlib.pyplot as plt
from scipy import stats

# Global variables
COHERENCE_TIME = 0.001 # ns
DETECTOR_EFFICIENCY = 0.03 # Fraction
MODE_INTENSITY = 10 # Photons per !!!SIMULATION_RESOLUTION!!!
SIMULATION_RESOLUTION = 0.0002 # ns

# Given the average photons per mode and sample size N, gives photons per bin for N bins for
# an amount of modes modes.
# Formula taken from: Mandel & Wolf, Optical Coherence and Quantum Optics, eq(13.3-29)
# Statistics option enables printing of some more information
def distribution_thermal_equilibrium(photon_average, modes, N, statistics = False):
    photons_n = np.arange(max([photon_average*10,100]))
    photons_chance = np.array([])
    for n in photons_n:
        photons_chance = append(photons_chance, math.factorial(n+modes-1)/(math.
            factorial(modes-1)*
            math.factorial(n))*1/((1+photon_average/modes)**modes*(1+modes/photon_average)
            **n))
    photons_distribution = stats.rv_discrete(values=(photons_n, photons_chance))
    if statistics == True:
        print('Median:', photons_distribution.moment(1), 'Variance:',
            photons_distribution.var())
        plot(photons_n, photons_distribution.cdf(photons_n))
        title('CDF of the distribution')
        xlabel('Photons, N')
        ylabel('Cumalitive probability')
        show()
    return photons_distribution.rvs(size=N)

# Distribution for picking the timescales on which the intensity will be variated given a
# coherence time.
# Returns N samples
def distribution_variation(coherence_time, N):
    variation_possible = np.arange(0, int(3*coherence_time/SIMULATION_RESOLUTION))
    return random.choice(variation_possible, size = N)

# Picks either 0 or 2 times the mode intensity. This gives a variance and mean of mode
# intensity, which is expected
# for thermal light. Returns N samples.
def distribution_intensity_thermal(N):
    return choice([0,2*MODE_INTENSITY], N)

# Given the average photons and sample size N returns the photons per bin for N bins
# coherent light using a poissoning distribution.
def distribution_coherent(photon_average, N):
    return stats.poisson(photon_average).rvs(size = N)

# Given a relative average photons and sample size N,
# gives the distribution for of N bins of single photons using an exponential distribution
# Assumed is that system is always in an excited state (only calculates the decays)
def distribution_single_photons(photon_average, N):
    photons = zeros(N, dtype = int)
```

```

photons_n = arange(150)
photons_chance = 1-exp(-photon_average*photons_n)
photons_chance = photons_chance/(sum(photons_chance))
photons_distribution = stats.rv_discrete(values=(photons_n,photons_chance))
i = 0
while i < N:
    photons[i] = photons[i]+1
    i = i+int(photons_distribution.rvs())
return photons

# Calculates how many coincidences there are between streamA and streamB for a delay tau
def coincidences(stream_a, stream_b, detection_time):
    tau_max = int(detection_time/SIMULATION_RESOLUTION)
    tau = np.arange(0, tau_max, dtype=int)
    photon_correlations = np.zeros(len(tau))
    for z in tau:
        photon_correlations[z] = np.sum(
            stream_a[0:-tau_max] *
            stream_b[z:z-tau_max]
        )
    return tau*SIMULATION_RESOLUTION, photon_correlations

# Simulates the effect of the beam splitter on the photon_stream. Returns two streams for the
two paths.
def beam_splitter(photon_stream):
    stream_a = np.random.binomial(photon_stream, 0.5)
    stream_b = photon_stream - stream_a
    return stream_a, stream_b

# Given an array of correlations, returns an estimate of the real measuring time
def measurement_time(tau, photon_correlations):
    time = sum(photon_correlations*tau) + sum(photon_correlations)*DETECTOR_DEAD_TIME
    print(str(time)+'_seconds')
    return time

# Simulates the effect of the detector efficiency on a photon stream. Given a detection
efficiency. Returns a stream
# of detection events (boolean array).
def detector_efficiency_effect(photon_stream, efficiency):
    efficiencies = np.zeros(len(photon_stream))
    efficiencies.fill(efficiency)
    return np.random.random(len(photon_stream)) - (1 - efficiencies) ** photon_stream > 0

# Runs the whole simulation for a given simulation duration (ns), simulation resolution (ps),
simulated intensity variations,
# detector resolution (ns) and and a combined runs_n. Has an option to print statistics about
the resulting photon stream.
def simulation(simul_duration, simul_resolution, simul_variatons, runs_n, statistics = False):
    simulated_correlations = zeros(int(simul_duration/simul_resolution)) # Initializes
simulated correlation array
    simulated_tau = arange(int(simul_duration/simul_resolution))*simul_resolution #
Initializes simulated tau array
    # Loop to apply i runs to the data, adds the new correlation data in the end
    for i in range(runs_n):
        time_variation = distribution_variation(COHERENCE_TIME, simul_variatons) #
Times to variate intensity
        intensities = distribution_intensity_thermal(simul_variatons) # Variated
intensities
        photon_stream = zeros(sum(time_variation), dtype= int) # Initializes photon
stream
        # Loop to make the photon stream for ii simulated intensity variations
        begin = 0
        for ii in range(len(time_variation)):
            photon_stream[begin:begin+time_variation[ii]] = distribution_coherent(
intensities[ii],time_variation[ii])

```

```

        begin += time_variation[ii]
    stream_a, stream_b = beam_splitter(photon_stream)
    stream_a = detector_efficiency_effect(stream_a, DETECTOR_EFFICIENCY)
    stream_b = detector_efficiency_effect(stream_b, DETECTOR_EFFICIENCY)
    tau, new_correlations = coincidences(stream_a, stream_b, simul_duration)
    simulated_correlations += new_correlations
if statistics == True:
    print('Average_photons_per_bin_(simul_res)_last_photon_stream:', average(
        photon_stream))
    print('Variation_photons_per_bin_(simul_res)_last_photon_stream:', var(
        photon_stream))
    print('Average_photons_per_bin_(simul_res)_last_photon_stream_detector_a,b:',
        average(stream_a), average(stream_b))
    print('Variation_photons_per_bin_(simul_res)_last_photon_stream_detector_a,b:'
        , var(stream_a), var(stream_b))
return simulated_tau, simulated_correlations

```